Search for the Lepton-Flavor-Violating Decays $B_s^0 \to \tau^\pm\mu^\mp$ and $B^0 \to \tau^\pm\mu^\mp$

R. Aaij *et al.*[*]
(LHCb Collaboration)

(Received 17 May 2019; published 22 November 2019)

Results are reported from a search for the rare decays $B_s^0 \to \tau^\pm\mu^\mp$ and $B^0 \to \tau^\pm\mu^\mp$, where the τ lepton is reconstructed in the channel $\tau^- \to \pi^-\pi^+\pi^-\nu_\tau$. These processes are effectively forbidden in the standard model, but they can potentially occur at detectable rates in models of new physics that can induce lepton-flavor-violating decays. The search is based on a data sample corresponding to 3 fb^{-1} of proton-proton collisions recorded by the LHCb experiment in 2011 and 2012. The event yields observed in the signal regions for both processes are consistent with the expected standard model backgrounds. Because of the limited mass resolution arising from the undetected τ neutrino, the B_s^0 and B^0 signal regions are highly overlapping. Assuming no contribution from $B^0 \to \tau^\pm\mu^\mp$, the upper limit $\mathcal{B}(B_s^0 \to \tau^\pm\mu^\mp) < 4.2 \times 10^{-5}$ is obtained at 95% confidence level. If no contribution from $B_s^0 \to \tau^\pm\mu^\mp$ is assumed, a limit of $\mathcal{B}(B^0 \to \tau^\pm\mu^\mp) < 1.4 \times 10^{-5}$ is obtained at 95% confidence level. These results represent the first limit on $\mathcal{B}(B_s^0 \to \tau^\pm\mu^\mp)$ and the most stringent limit on $\mathcal{B}(B^0 \to \tau^\pm\mu^\mp)$.

DOI: 10.1103/PhysRevLett.123.211801

Lepton-flavor-violating decays of mesons containing b quarks, such as $B^0(b\bar{d}) \to \tau^\pm\mu^\mp$ and $B_s^0(b\bar{s}) \to \tau^\pm\mu^\mp$, are extremely suppressed in the standard model (SM), with expected branching fractions of order 10^{-54} [1]. (The inclusion of charge-conjugate processes is implied throughout this Letter.) These processes involve not only quantum loops but also neutrino oscillations. Signals at the level expected in the SM lie far below current and foreseen experimental sensitivities. However, many theoretical models proposed to explain possible experimental tensions observed in other B-meson decays (discussed below) naturally allow for branching fractions that are within current sensitivity. Among them, models containing a heavy neutral gauge boson (Z') could lead to a $B_s^0 \to \tau^\pm\mu^\mp$ branching fraction of up to 10^{-8} [2,3] when only left-handed or right-handed couplings to quarks are considered, or of the order of 10^{-6} [3] if both are allowed. In models with either scalar or vector leptoquarks, the largest predictions for the $B_s^0 \to \tau^\pm\mu^\mp$ branching fraction range from 10^{-9} to 10^{-5}, depending on the assumed leptoquark mass [4–6]. The three-site Pati-Salam gauge model favors values for this branching fraction in the range 10^{-4}–10^{-6} [7,8].

The SM predicts that the electroweak couplings for the three lepton families are universal, a result referred to as lepton-flavor universality (LFU). Experimental tests of LFU performed using $b \to s\ell^+\ell^-$ and $b \to c\ell^-\bar{\nu}$ processes show tensions with respect to the SM predictions for the observables $R_{K^{(*)}}$ [9,10] and $\mathcal{R}(D^{(*)})$ [11]. For the latter, the observed discrepancy with respect to the SM prediction is greater than 3 standard deviations. Because theoretical models that can account for the possible LFU effects observed in data often predict lepton-flavor violation (LFV) as well [12], searches for LFV processes provide a powerful signature for probing these models.

An upper limit $\mathcal{B}(B^0 \to \tau^\pm\mu^\mp) < 2.2 \times 10^{-5}$ at 90% confidence level (C.L.) was obtained by the *BABAR* Collaboration [13]. There are currently no experimental results for the $B_s^0 \to \tau^\pm\mu^\mp$ mode.

This Letter reports results from the first search for the decay $B_s^0 \to \tau^\pm\mu^\mp$, along with the most stringent limit on the process $B^0 \to \tau^\pm\mu^\mp$. The analysis is performed on data corresponding to an integrated luminosity of 3 fb^{-1} of proton-proton (pp) collisions, recorded with the LHCb detector during the years 2011 and 2012 at center-of-mass energies of 7 and 8 TeV, respectively. The τ leptons are reconstructed through the decay $\tau^- \to \pi^-\pi^+\pi^-\nu_\tau$, which mainly proceeds via the production of two intermediate resonances, $a_1(1260)^- \to \pi^+\pi^-\pi^-$ and $\rho(770)^0 \to \pi^+\pi^-$ [14], which help in the signal selection. In this mode, the τ decay vertex can be precisely reconstructed, facilitating a good reconstruction of the B-meson invariant mass despite the undetected neutrino. To avoid experimenter bias, the B-meson invariant-mass signal region was not examined until the selection and fit procedures were finalized. The signal yield is determined by performing an unbinned maximum-likelihood fit to the reconstructed B-meson invariant-mass

[*]Full author list given at the end of the article.

Published by the American Physical Society under the terms of the Creative Commons Attribution 4.0 International license. Further distribution of this work must maintain attribution to the author(s) and the published article's title, journal citation, and DOI. Funded by SCOAP[3].

 © 2019 CERN, for the LHCb Collaboration

distribution and is converted into a branching fraction using the decay $B^0 \to D^-(\to K^+\pi^-\pi^-)\pi^+$ as a normalization channel.

The LHCb detector [15,16] is a single-arm forward spectrometer covering the pseudorapidity range $2 < \eta < 5$, designed for the study of particles containing b or c quarks. The detector includes a high-precision tracking system consisting of a silicon-strip vertex detector surrounding the pp interaction region, a large-area silicon-strip detector located upstream of a dipole magnet with a bending power of about 4 Tm, and three stations of silicon-strip detectors and straw drift tubes placed downstream of the magnet. The tracking system provides a measurement of the momentum, p, of charged particles with a relative uncertainty varying from 0.5% at low momentum to 1.0% at 200 GeV/c. The minimum distance of a track to a primary vertex (PV), the impact parameter (IP), is measured with a resolution of $(15 + 29/p_T)$ μm, where p_T is the component of the momentum transverse to the beam, in GeV/c. Different types of charged hadrons are distinguished using information from two ring-imaging Cherenkov detectors. Photons, electrons, and hadrons are identified by a calorimeter system consisting of scintillating-pad and preshower detectors, an electromagnetic and a hadronic calorimeter. Muons are identified by a system composed of alternating layers of iron and multiwire proportional chambers.

The on-line event selection is performed by a trigger [17] consisting of a hardware stage based on information from the calorimeter and muon systems, followed by a software stage, which performs a full event reconstruction. At the hardware trigger stage, signal candidates are required to have a muon with high p_T, while, for the normalization sample, events are required to have a hadron with high transverse energy in the calorimeters. The software trigger requires a two-, three-, or four-track secondary vertex with a significant displacement from any primary pp interaction vertex. A multivariate algorithm [18] is used to identify secondary vertices consistent with the decay of a b hadron. At least one charged particle must have a transverse momentum $p_T > 1.0(1.6)$ GeV/c for muons (hadrons) and must be inconsistent with originating from a PV.

Simulation is used to optimize the selection, determine the signal model for the fit, and obtain the selection efficiencies. In the simulation, pp collisions are generated using PYTHIA [19] with a specific LHCb configuration [20]. The τ decay is simulated using the TAUOLA decay library tuned with *BABAR* data [21], while the decays of all other unstable particles are described by EVTGEN [22]. Final-state radiation is accounted for using PHOTOS [23]. The interaction of the generated particles with the detector, and its response, are implemented using the GEANT4 toolkit [24], as described in Ref. [25].

Both signal and normalization candidates are formed using tracks that are inconsistent with originating from any PV. Candidate $\tau^- \to \pi^-\pi^+\pi^-\nu_\tau$ and $D^- \to K^+\pi^-\pi^-$ decays are reconstructed from three tracks forming a good-quality vertex and with particle identification information corresponding to their assumed particle hypotheses. Candidate $B^0_{(s)} \to \tau^\pm\mu^\mp$ decays are formed by combining a reconstructed τ lepton and an oppositely charged track identified as a muon. A control sample of same-sign candidates, which are formed by a τ lepton and a muon with identical charges, is also selected to serve, during the selection process, as a proxy for the large component of the background in which the muon and the τ candidate charges are uncorrelated. For the normalization mode, $B^0 \to D^-\pi^+$ candidates are made out of a reconstructed D meson and an oppositely charged track identified as a pion. The decay vertex of the signal or normalization B candidate is determined through a fit to all reconstructed particles in the decay chain [26], which is required to be of good quality. The B-meson p_T is required to be greater than 5 GeV/c for both signal and normalization modes.

While the neutrino from the τ decay escapes detection, its momentum vector can be constrained from the measured positions of the primary and τ decay vertices, the momenta of the muon and the three pions, and the trajectory of the muon. Then, by imposing the requirements that the mass of the system formed from the three pions and the unobserved neutrino corresponds to the mass of the τ lepton, and by requiring that the B decay vertex lies on the trajectories of the muon, of the τ lepton, and of the B meson, the invariant mass of the $B^0_{(s)}$ candidate can be determined analytically up to a twofold ambiguity. Because of the quadratic nature of the equation, the computed masses may be unphysical. This occurs in 32% of the selected signal in the simulated event sample due to measurement resolutions, and in 48% of the same-sign candidates in data. These candidates are removed, thereby improving the signal-to-background ratio. The solution whose distribution shows the largest separation between signal and background is used as the reconstructed B invariant mass, M_B, in the analysis. The distributions of M_B for candidates satisfying the previously described initial selection in the simulated signal samples and in the opposite-sign control sample in the data are shown in Fig. 1.

To reduce the data to a manageable level and focus on the rejection of the most difficult backgrounds, the low-mass region with $M_B < 4$ GeV/c^2 is discarded. The signal loss due to this requirement is negligible.

To further reduce the background, additional requirements, optimized with same-sign candidates and simulated samples, are applied to the selected $B^0_{(s)} \to \tau^\pm\mu^\mp$ decays. Taking advantage of the resonant structure of the $\tau^- \to \pi^-\pi^+\pi^-\nu_\tau$ decay, candidates with both combinations of oppositely charged pions with invariant masses below 550 MeV/c^2 are removed. Candidates with a three-pion invariant mass greater than 1.8 GeV/c^2 are

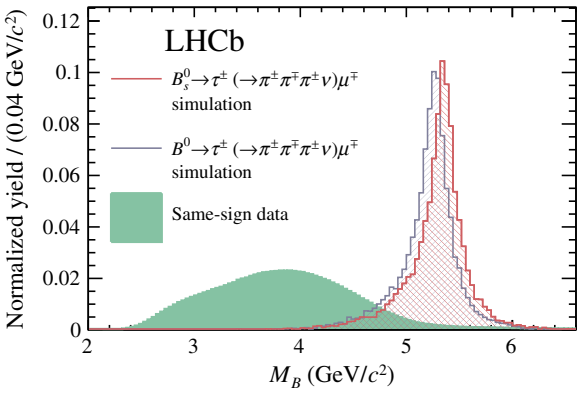

FIG. 1. Normalized distributions of the reconstructed invariant mass for B_s^0 and B^0 in simulated event samples and for same-sign candidates in data, after applying the initial event selection (see the text).

discarded to veto the background contribution due to $D^+ \to \pi^+\pi^-\pi^+$ decays.

A set of isolation variables is used to reduce background from decays with additional reconstructed particles. The first class of isolation variables exploits the presence of activity in the calorimeter to identify the contribution of neutral particles contained in a cone centered on the B or τ flight directions. The second class is based on the presence of additional tracks consistent with originating from the B or τ decay vertices, or uses a multivariate classifier, trained on simulated data, to discriminate against candidates whose decay products are compatible with forming good-quality vertices with other tracks in the event. These variables are combined using a boosted decision tree (BDT) [27], trained on same-sign candidates and simulated $B_s^0 \to \tau^\pm\mu^\mp$ decays. Candidates with a BDT output compatible with that of background are discarded. A second BDT is used to reduce to a negligible level the contribution of combinatorial background, which extends over the whole mass range but dominates at higher masses. It uses variables related to vertex quality and reconstructed particle opening angles and is trained on samples of same-sign candidates with $M_B > 6.2$ GeV/c^2 and simulated $B_s^0 \to \tau^\pm\mu^\mp$ decays.

Some background processes, such as $B_{(s)}^0 \to D_{(s)}^-(\to \mu^-\bar{\nu}_\mu)\pi^+\pi^-\pi^+$, have M_B distributions peaking in the signal region. In these decays, the three pions come from the B decay vertex, and therefore the reconstructed B and τ decay vertices are very close. Discarding candidates with a reconstructed τ decay-time significance lower than 1.8 reduces this type of background to a negligible level while keeping ∼75% of the signal, according to studies performed on simulation. All previously described selection criteria also suppress a possible contribution from the $B^0 \to a_1(1260)^-\mu^+\nu_\mu$ mode, whose selection efficiency is 60 times lower than that of the signal. Its rate is currently unmeasured, but, given that the largest known $b \to u$ semileptonic decay branching fractions are of the order of 10^{-4}, its branching fraction is not expected to be much higher. Events from the decay $\tau^- \to \pi^-\pi^+\pi^-\pi^0\nu_\tau$ passing the selection are also included as signal.

The selection procedure retains 17 746 candidates. According to studies based on simulations, the remaining background is dominated by $B_{(s)}^0 \to D_{(s)}^{(*)}\mu\nu X$ decays.

The selection efficiencies for the signal and normalization modes, $\epsilon_{B_{(s)}^0\to\tau\mu}$ and $\epsilon_{B\to D\pi}$, respectively, are estimated using simulation or, whenever possible, data. The efficiency $\epsilon_{B_{(s)}^0\to\tau\mu}$ includes those for both $\tau^- \to \pi^-\pi^+\pi^-\nu_\tau$ and $\tau^- \to \pi^-\pi^+\pi^-\pi^0\nu_\tau$ decays, where the latter is weighted by the ratio of the two branching fractions. The $\tau^- \to \pi^-\pi^+\pi^-\pi^0\nu_\tau$ channel contributes by ∼16% to the extracted signal yield. The tracking and particle identification efficiencies are determined using data [28,29]. The trigger efficiency for the normalization channel is estimated using a trigger-unbiased subsample made of events which have been triggered independently of the normalization candidate. For the signal, muons from $B^+ \to J/\psi(\to \mu^+\mu^-)K^+$ decays are used to evaluate the muon trigger efficiency, and corrections are applied to the simulated signal samples. To account for differences between the control and the signal samples, the efficiency is computed as a function of the muon p_T and IP. Simulation as well as $B^+ \to J/\psi(\to \mu^+\mu^-)K^+$ decays is used to determine the software-trigger efficiency and its systematic uncertainty.

The signal yield for the normalization mode is obtained from a fit to the invariant-mass distribution of the $B^0 \to D^-\pi^+$ candidates. In the fit the signal is modeled by the sum of two crystal ball (CB) [30] functions, with tails on opposite sides, having common means and widths, but independent tail parameters. The tail parameters are fixed to values determined from a fit to a sample of $B^0 \to D^-(\to K^+\pi^-\pi^-)\pi^+$ simulated decays, while all other parameters are left free. The small background contribution is described by an exponential function. The measured yield of the $B^0 \to D^-\pi^+$ mode is $N^{\rm norm} = 22588 \pm 176$, where the uncertainty is statistical only.

The $B_{(s)}^0 \to \tau^\pm\mu^\mp$ branching fractions can be written as

$$\mathcal{B}\left(B_{(s)}^0 \to \tau^\pm\mu^\mp\right) = \alpha_{(s)}^{\rm norm} N_{(s)}^{\rm sig}, \tag{1}$$

where $N_{(s)}^{\rm sig}$ is the number of observed $B_{(s)}^0 \to \tau^\pm\mu^\mp$ decays and $\alpha_{(s)}^{\rm norm}$ a normalization factor. The latter is defined by

$$\alpha_{(s)}^{\rm norm} = \frac{f_{B^0}}{f_{B_{(s)}^0}} \frac{\mathcal{B}[B^0 \to D^-(\to K^+\pi^-\pi^-)\pi^+]}{\mathcal{B}(\tau^- \to \pi^-\pi^+\pi^-\nu_\tau)} \frac{\epsilon_{B\to D\pi}}{\epsilon_{B_{(s)}^0\to\tau\mu}} \frac{1}{N^{\rm norm}}, \tag{2}$$

using externally measured quantities: the ratio of b-quark hadronization fractions to B_s^0 and B^0 mesons, $f_{B_s^0}/f_{B^0} = 0.259 \pm 0.015$ [31], $\mathcal{B}[B^0 \to D^-(\to K^+\pi^-\pi^-)\pi^+] = (2.26 \pm 0.14) \times 10^{-4}$ [32] and $\mathcal{B}(\tau^- \to \pi^-\pi^+\pi^-\nu_\tau) = (9.02 \pm 0.05)\%$ [32]. The measured values of $\alpha_{(s)}^{\rm norm}$ for the B_s^0 and B^0 modes are, respectively,

$$\alpha_s^{\rm norm} = (4.32 \pm 0.19 \pm 0.45 \pm 0.36) \times 10^{-7},$$
$$\alpha^{\rm norm} = (1.25 \pm 0.06 \pm 0.13 \pm 0.08) \times 10^{-7}, \quad (3)$$

where the three quoted uncertainties are the statistical uncertainty due to the sizes of the signal and normalization simulated and data samples, the systematic uncertainty on the selection efficiencies (dominated by the trigger efficiency contribution, ∼11%), and the total uncertainty on the externally measured quantities.

A final BDT is built to split the selected candidates into four samples with different signal-to-background ratios. It combines 16 discriminating variables, none of which are correlated with the B-meson invariant mass. The most important ones are the invariant masses of the three-pion system and of the two combinations of oppositely charged pions, the B-meson IP and flight distance significances, and the output of the BDT based on isolation variables. The output of the BDT is transformed to have a uniform distribution between 0 and 1 for $B_s^0 \to \tau^\pm(\to \pi^\pm\pi^\mp\pi^\pm\nu_\tau)\mu^\mp$ simulated decays. As a consequence, its distribution for the background peaks at low BDT values. All samples are divided into four bins of equal width in BDT output. Their distributions are shown in Fig. 2.

The signal yield is evaluated by performing a simultaneous unbinned maximum-likelihood fit to the M_B distributions in the range $[4.6, 5.8]$ GeV/c^2 of the four samples corresponding to different BDT bins. In each bin, the data are described by the sum of a signal and a background component. The background shape is modeled by the upper tail of a reversed CB function, whose peak position and tail parameters are shared among BDT bins. For the determination of the systematic uncertainties, different sets of constrained parameters or alternative background models, such as the sum of two Gaussian functions, are considered. The signal shapes are described by double-sided Hypatia functions [33] whose parameters are initialized to the values obtained from a fit to the $B_s^0 \to \tau^\pm\mu^\mp$ and $B^0 \to \tau^\pm\mu^\mp$ simulated samples and allowed to vary within Gaussian constraints accounting for possible discrepancies between data and simulation. The width of the Hypatia functions are ∼330 MeV/c^2 for both signal modes in the most sensitive BDT bin. As the separation between $B_s^0 \to \tau^\pm\mu^\mp$ and $B^0 \to \tau^\pm\mu^\mp$ signal shapes is limited, two independent fits are performed while assuming the contribution of either the B_s^0 or the B^0 signal only. The signal fractional yields in each BDT bin are Gaussian constrained according to their expected values and uncertainties. The fit result corresponding to the hypothesis of the B_s^0 signal only is shown in Fig. 3. The fit procedure is validated by performing fits to a set of pseudoexperiments where the mass distributions are randomly generated according to the background model observed in the data. The pulls of all fitted parameters are normally distributed, except those of the signal yields $N^{\rm sig}$, which have the expected widths but exhibit a very small bias of -3 ± 1 (2 ± 2) events for the B_s^0 (B^0) mode. This effect is accounted for by adding the bias to $N^{\rm sig}$ in the simultaneous fits to the four BDT regions for both B^0 and B_s^0. The obtained signal yields are

$$N^{\rm sig}_{B_s^0 \to \tau^\pm\mu^\mp} = -16 \pm 38,$$
$$N^{\rm sig}_{B^0 \to \tau^\pm\mu^\mp} = -65 \pm 58,$$

where the uncertainties account for the statistical ones as well as those on the signal and background shape parameters. They show no evidence of any signal excess.

Using the calculated values of the normalization factors $\alpha^{\rm norm}$ and $\alpha_s^{\rm norm}$ from Eq. (1) together with Eq. (3), the observed yields from the likelihood fits are translated into upper limits on the branching fractions using the CL_s method [34,35]. The total uncertainty on the normalization factor is accounted for as an additional Gaussian constraint in the simultaneous fit. Furthermore, a systematic uncertainty on the signal yield of 34 (41) for the B_s^0 (B^0) mode, derived using different sets of constrained parameters or alternative background models, is added to account for the uncertainties in the background shape. The expected and observed CL_s values as a function of the branching fraction are shown in the Supplemental Material [36]. The corresponding limits on the B_s^0 and B^0 branching fractions at 90% and 95% C.L. are given in Table I assuming a

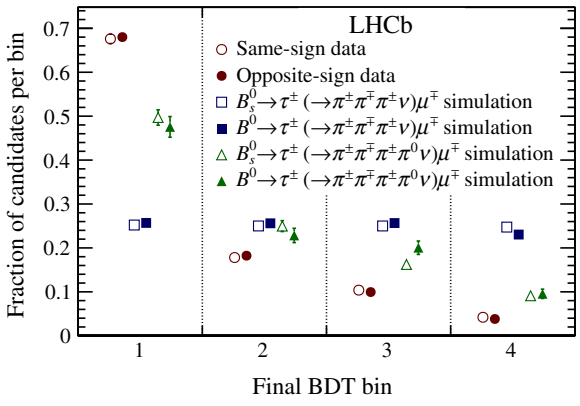

FIG. 2. Final BDT output binned distributions for data and simulated signal samples. The markers are displaced horizontally to improve visibility.

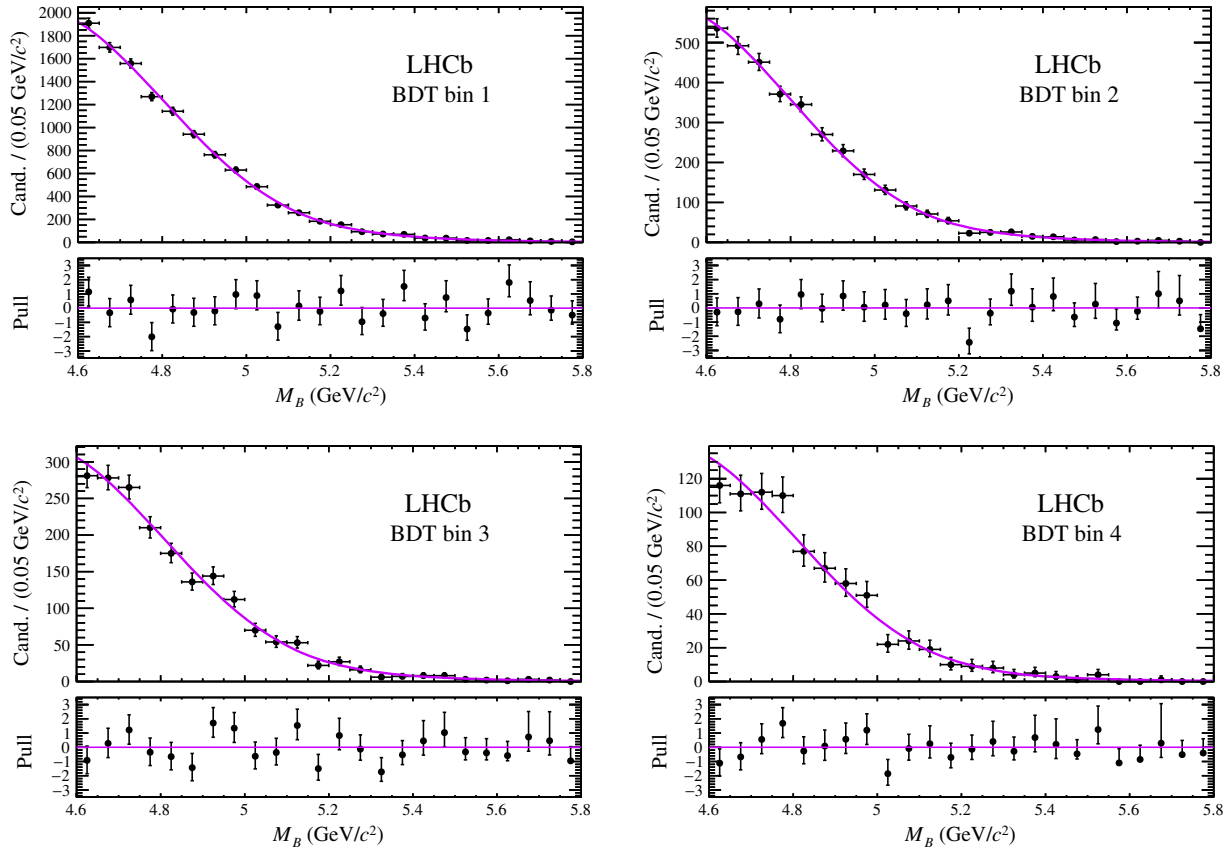

FIG. 3. Distributions of the reconstructed B invariant mass in data in the four final BDT bins with the projections of the fit for the B_s^0 signal-only hypothesis overlaid. The lower part of each figure shows the normalized residuals.

negligible contribution from the $B^0 \to a_1(1260)^- \mu^+ \nu_\mu$ mode. A possible residual contribution of this background would lower the expected limits by $\sim 16\% \times \{\mathcal{B}[B^0 \to a_1(1260)^- \mu^+ \nu_\mu]/10^{-4}\}$. The impact of systematic uncertainties on the final limits is about 35%, dominated by the uncertainty on the background model.

These results represent the best upper limits to date. They constitute a factor ~ 2 improvement with respect to the *BABAR* result for the B^0 mode [13] and the first measurement for the B_s^0 mode. The allowed range on the $B_s^0 \to \tau^\pm \mu^\mp$ branching fraction preferred by the three-site Pati-Salam model [7,8] is significantly reduced by the results presented in this Letter.

TABLE I. Expected and observed 90% and 95% C.L. limits on the $B_{(s)}^0 \to \tau^\pm \mu^\mp$ branching fraction.

Mode	Limit	90% C.L.	95% C.L.
$B_s^0 \to \tau^\pm \mu^\mp$	Observed	3.4×10^{-5}	4.2×10^{-5}
	Expected	3.9×10^{-5}	4.7×10^{-5}
$B^0 \to \tau^\pm \mu^\mp$	Observed	1.2×10^{-5}	1.4×10^{-5}
	Expected	1.6×10^{-5}	1.9×10^{-5}

We express our gratitude to our colleagues in the CERN accelerator departments for the excellent performance of the LHC. We thank the technical and administrative staff at the LHCb institutes. We acknowledge support from CERN and from the national agencies: CAPES, CNPq, FAPERJ, and FINEP (Brazil); MOST and NSFC (China); CNRS/IN2P3 (France); BMBF, DFG, and MPG (Germany); INFN (Italy); NWO (Netherlands); MNiSW and NCN (Poland); MEN/IFA (Romania); MSHE (Russia); MinECo (Spain); SNSF and SER (Switzerland); NASU (Ukraine); STFC (United Kingdom); DOE NP and NSF (USA). We acknowledge the computing resources that are provided by CERN, IN2P3 (France), KIT and DESY (Germany), INFN (Italy), SURF (Netherlands), PIC (Spain), GridPP (United Kingdom), RRCKI and Yandex LLC (Russia), CSCS (Switzerland), IFIN-HH (Romania), CBPF (Brazil), PL-GRID (Poland), and OSC (USA). We are indebted to the communities behind the multiple open-source software packages on which we depend. Individual groups or members have received support from the AvH Foundation (Germany); EPLANET, Marie Skłodowska-Curie Actions and ERC (European Union); ANR, Labex P2IO and OCEVU, and Région Auvergne-Rhône-Alpes (France); the Key Research Program of Frontier Sciences of CAS,

CAS PIFI, and the Thousand Talents Program (China); RFBR, RSF, and Yandex LLC (Russia); GVA, XuntaGal, and GENCAT (Spain); and the Royal Society and the Leverhulme Trust (United Kingdom).

[1] L. Calibbi and G. Signorelli, Charged lepton flavour violation: An experimental and theoretical introduction, Riv. Nuovo Cimento **41**, 71 (2018).

[2] D. Bečirević, O. Sumensari, and R. Z. Funchal, Lepton flavor violation in exclusive $b \to s$ decays, Eur. Phys. J. C **76**, 134 (2016).

[3] A. Crivellin, L. Hofer, J. Matias, U. Nierste, S. Pokorski, and J. Rosiek, Lepton-flavor violating B decays in generic Z' models, Phys. Rev. D **92**, 054013 (2015).

[4] I. de Medeiros Varzielas and G. Hiller, Clues for flavor from rare lepton and quark decays, J. High Energy Phys. 06 (2015) 072.

[5] D. Bečirević, N. Košnik, O. Sumensari, and R. Zukanovich Funchal, Palatable leptoquark scenarios for lepton flavor violation in exclusive $b \to s\ell_1\ell_2$ modes, J. High Energy Phys. 11 (2016) 035.

[6] A. D. Smirnov, Vector leptoquark mass limits and branching ratios of $K_L^0, B^0, B_s \to l_i^+ l_j^-$ decays with account of fermion mixing in leptoquark currents, Mod. Phys. Lett. A **33**, 1850019 (2018).

[7] M. Bordone, C. Cornella, J. Fuentes-Martín, and G. Isidori, Low-energy signatures of the PS^3 model: From B-physics anomalies to LFV, J. High Energy Phys. 10 (2018) 148.

[8] C. Cornella, J. Fuentes-Martin, and G. Isidori, Revisiting the vector leptoquark explanation of the B-physics anomalies, J. High Energy Phys. 07 (2019) 168.

[9] R. Aaij *et al.* (LHCb Collaboration), Test of lepton universality with $B^0 \to K^{*0}\ell^+\ell^-$ decays, J. High Energy Phys. 08 (2017) 055.

[10] R. Aaij *et al.* (LHCb Collaboration), Search for Lepton-Universality Violation in $B^+ \to K^+\ell^+\ell^-$ Decays, Phys. Rev. Lett. **122**, 191801 (2019).

[11] Y. Amhis *et al.* (Heavy Flavor Averaging Group), Averages of b-hadron, c-hadron, and τ-lepton properties as of summer 2016, Eur. Phys. J. C **77**, 895 (2017); updated results and plots are available at https://hflav.web.cern.ch.

[12] S. L. Glashow, D. Guadagnoli, and K. Lane, Lepton Flavor Violation in B Decays?, Phys. Rev. Lett. **114**, 091801 (2015).

[13] B. Aubert *et al.* (*BABAR* Collaboration), Searches for the decays $B^0 \to \ell^\pm\tau^\mp$ and $B^+ \to \ell^+\nu$ ($\ell = \mathrm{e}, \mu$) using hadronic tag reconstruction, Phys. Rev. D **77**, 091104 (2008).

[14] S. Schael *et al.* (ALEPH Collaboration), Branching ratios and spectral functions of τ decays: Final ALEPH measurements and physics implications, Phys. Rep. **421**, 191 (2005).

[15] A. A. Alves, Jr. *et al.* (LHCb Collaboration), The LHCb detector at the LHC, J. Instrum. **3**, S08005 (2008).

[16] R. Aaij *et al.* (LHCb Collaboration), LHCb detector performance, Int. J. Mod. Phys. A **30**, 1530022 (2015).

[17] R. Aaij *et al.*, The LHCb trigger and its performance in 2011, J. Instrum. **8**, P04022 (2013).

[18] V. V. Gligorov and M. Williams, Efficient, reliable and fast high-level triggering using a bonsai boosted decision tree, J. Instrum. **8**, P02013 (2013).

[19] T. Sjöstrand, S. Mrenna, and P. Skands, PYTHIA6.4 physics and manual, J. High Energy Phys. 05 (2006) 026; A brief introduction to PYTHIA8.1, Comput. Phys. Commun. **178**, 852 (2008).

[20] I. Belyaev *et al.*, Handling of the generation of primary events in Gauss, the LHCb simulation framework, J. Phys. Conf. Ser. **331**, 032047 (2011).

[21] I. M. Nugent, T. Przedziński, P. Roig, O. Shekhovtsova, and Z. Wąs, Resonance chiral Lagrangian currents and experimental data for $\tau^- \to \pi^-\pi^-\pi^+\nu_\tau$, Phys. Rev. D **88**, 093012 (2013).

[22] D. J. Lange, The EVTGEN particle decay simulation package, Nucl. Instrum. Methods Phys. Res., Sect. A **462**, 152 (2001).

[23] P. Golonka and Z. Was, PHOTOS Monte Carlo: A precision tool for QED corrections in Z and W decays, Eur. Phys. J. C **45**, 97 (2006).

[24] J. Allison *et al.* (GEANT4 Collaboration), GEANT4 developments and applications, IEEE Trans. Nucl. Sci. **53**, 270 (2006); S. Agostinelli *et al.* (GEANT4 Collaboration), GEANT4: A simulation toolkit, Nucl. Instrum. Methods Phys. Res., Sect. A **506**, 250 (2003).

[25] M. Clemencic, G. Corti, S. Easo, C. R. Jones, S. Miglioranzi, M. Pappagallo, and P. Robbe, The LHCb simulation application, GAUSS: Design, evolution and experience, J. Phys. Conf. Ser. **331**, 032023 (2011).

[26] W. D. Hulsbergen, Decay chain fitting with a Kalman filter, Nucl. Instrum. Methods Phys. Res., Sect. A **552**, 566 (2005).

[27] L. Breiman, J. H. Friedman, R. A. Olshen, and C. J. Stone, *Classification and Regression Trees* (Wadsworth International Group, Belmont, CA, 1984).

[28] R. Aaij *et al.* (LHCb Collaboration), Measurement of the track reconstruction efficiency at LHCb, J. Instrum. **10**, P02007 (2015).

[29] L. Anderlini *et al.*, The PIDCalib package, LHCb Report No. LHCb-PUB-2016-021, 2016.

[30] T. Skwarnicki, A study of the radiative cascade transitions between the Upsilon-prime and Upsilon resonances, Ph.D. thesis, Institute of Nuclear Physics, 1986 [DESY Report No. DESY-F31-86-02, 1986].

[31] R. Aaij *et al.* (LHCb Collaboration), Measurement of the fragmentation fraction ratio f_s/f_d and its dependence on B meson kinematics, J. High Energy Phys. 04 (2013) 001; the f_s/f_d value was updated in LHCb Report No. LHCb-CONF-2013-011, 2013.

[32] M. Tanabashi *et al.* (Particle Data Group), Review of particle physics, Phys. Rev. D **98**, 030001 (2018).

[33] D. Martínez Santos and F. Dupertuis, Mass distributions marginalized over per-event errors, Nucl. Instrum. Methods Phys. Res., Sect. A **764**, 150 (2014).

[34] A. L. Read, Presentation of search results: The CL_s technique, J. Phys. G **28**, 2693 (2002).

[35] G. Cowan, K. Cranmer, E. Gross, and O. Vitells, Asymptotic formulae for likelihood-based tests of new physics, Eur. Phys. J. C **71**, 1554 (2011).

[36] See Supplemental Material at http://link.aps.org/supplemental/10.1103/PhysRevLett.123.211801 for the expected and observed CLs as a function of the $B^0 \to \tau^\pm\mu^\mp$ and $B_s^0 \to \tau^\pm\mu^\mp$ branching fractions.

R. Aaij,[29] C. Abellán Beteta,[46] B. Adeva,[43] M. Adinolfi,[50] C. A. Aidala,[78] Z. Ajaltouni,[7] S. Akar,[61] P. Albicocco,[20] J. Albrecht,[12] F. Alessio,[44] M. Alexander,[55] A. Alfonso Albero,[42] G. Alkhazov,[35] P. Alvarez Cartelle,[57] A. A. Alves Jr.,[43] S. Amato,[2] Y. Amhis,[9] L. An,[19] L. Anderlini,[19] G. Andreassi,[45] M. Andreotti,[18] J. E. Andrews,[62] F. Archilli,[20] J. Arnau Romeu,[8] A. Artamonov,[41] M. Artuso,[64] K. Arzymatov,[39] E. Aslanides,[8] M. Atzeni,[46] B. Audurier,[24] S. Bachmann,[14] J. J. Back,[52] S. Baker,[57] V. Balagura,[9,b] W. Baldini,[18,44] A. Baranov,[39] R. J. Barlow,[58] S. Barsuk,[9] W. Barter,[57] M. Bartolini,[21] F. Baryshnikov,[74] V. Batozskaya,[33] B. Batsukh,[64] A. Battig,[12] V. Battista,[45] A. Bay,[45] F. Bedeschi,[26] I. Bediaga,[1] A. Beiter,[64] L. J. Bel,[29] V. Belavin,[39] S. Belin,[24] N. Beliy,[4] V. Bellee,[45] K. Belous,[41] I. Belyaev,[36] G. Bencivenni,[20] E. Ben-Haim,[10] S. Benson,[29] S. Beranek,[11] A. Berezhnoy,[37] R. Bernet,[46] D. Berninghoff,[14] E. Bertholet,[10] A. Bertolin,[25] C. Betancourt,[46] F. Betti,[17,c] M. O. Bettler,[51] Ia. Bezshyiko,[46] S. Bhasin,[50] J. Bhom,[31] M. S. Bieker,[12] S. Bifani,[49] P. Billoir,[10] A. Birnkraut,[12] A. Bizzeti,[19,d] M. Bjørn,[59] M. P. Blago,[44] T. Blake,[52] F. Blanc,[45] S. Blusk,[64] D. Bobulska,[55] V. Bocci,[28] O. Boente Garcia,[43] T. Boettcher,[60] A. Bondar,[40,e] N. Bondar,[35] S. Borghi,[58,44] M. Borisyak,[39] M. Borsato,[14] M. Boubdir,[11] T. J. V. Bowcock,[56] C. Bozzi,[18,44] S. Braun,[14] A. Brea Rodriguez,[43] M. Brodski,[44] J. Brodzicka,[31] A. Brossa Gonzalo,[52] D. Brundu,[24,44] E. Buchanan,[50] A. Buonaura,[46] C. Burr,[58] A. Bursche,[24] J. S. Butter,[29] J. Buytaert,[44] W. Byczynski,[44] S. Cadeddu,[24] H. Cai,[68] R. Calabrese,[18,f] S. Cali,[20] R. Calladine,[49] M. Calvi,[22,g] M. Calvo Gomez,[42,h] A. Camboni,[42,h] P. Campana,[20] D. H. Campora Perez,[44] L. Capriotti,[17,c] A. Carbone,[17,c] G. Carboni,[27] R. Cardinale,[21] A. Cardini,[24] P. Carniti,[22,g] K. Carvalho Akiba,[2] A. Casais Vidal,[43] G. Casse,[56] M. Cattaneo,[44] G. Cavallero,[21] R. Cenci,[26,i] M. G. Chapman,[50] M. Charles,[10,44] Ph. Charpentier,[44] G. Chatzikonstantinidis,[49] M. Chefdeville,[6] V. Chekalina,[39] C. Chen,[3] S. Chen,[24] S.-G. Chitic,[44] V. Chobanova,[43] M. Chrzaszcz,[44] A. Chubykin,[35] P. Ciambrone,[20] X. Cid Vidal,[43] G. Ciezarek,[44] F. Cindolo,[17] P. E. L. Clarke,[54] M. Clemencic,[44] H. V. Cliff,[51] J. Closier,[44] J. L. Cobbledick,[58] V. Coco,[44] J. A. B. Coelho,[9] J. Cogan,[8] E. Cogneras,[7] L. Cojocariu,[34] P. Collins,[44] T. Colombo,[44] A. Comerma-Montells,[14] A. Contu,[24] G. Coombs,[44] S. Coquereau,[42] G. Corti,[44] C. M. Costa Sobral,[52] B. Couturier,[44] G. A. Cowan,[54] D. C. Craik,[60] A. Crocombe,[52] M. Cruz Torres,[1] R. Currie,[54] C. L. Da Silva,[63] E. Dall'Occo,[29] J. Dalseno,[43,j] C. D'Ambrosio,[44] A. Danilina,[36] P. d'Argent,[14] A. Davis,[58] O. De Aguiar Francisco,[44] K. De Bruyn,[44] S. De Capua,[58] M. De Cian,[45] J. M. De Miranda,[1] L. De Paula,[2] M. De Serio,[16,k] P. De Simone,[20] J. A. de Vries,[29] C. T. Dean,[55] W. Dean,[78] D. Decamp,[6] L. Del Buono,[10] B. Delaney,[51] H.-P. Dembinski,[13] M. Demmer,[12] A. Dendek,[32] D. Derkach,[75] O. Deschamps,[7] F. Desse,[9] F. Dettori,[24] B. Dey,[69] A. Di Canto,[44] P. Di Nezza,[20] S. Didenko,[74] H. Dijkstra,[44] F. Dordei,[24] M. Dorigo,[26,l] A. C. dos Reis,[1] A. Dosil Suárez,[43] L. Douglas,[55] A. Dovbnya,[47] K. Dreimanis,[56] L. Dufour,[44] G. Dujany,[10] P. Durante,[44] J. M. Durham,[63] D. Dutta,[58] R. Dzhelyadin,[41,a] M. Dziewiecki,[14] A. Dziurda,[31] A. Dzyuba,[35] S. Easo,[53] U. Egede,[57] V. Egorychev,[36] S. Eidelman,[40,e] S. Eisenhardt,[54] U. Eitschberger,[12] R. Ekelhof,[12] S. Ek-In,[45] L. Eklund,[55] S. Ely,[64] A. Ene,[34] S. Escher,[11] S. Esen,[29] T. Evans,[61] A. Falabella,[17] C. Färber,[44] N. Farley,[49] S. Farry,[56] D. Fazzini,[9] M. Féo,[44] P. Fernandez Declara,[44] A. Fernandez Prieto,[43] F. Ferrari,[17,c] L. Ferreira Lopes,[45] F. Ferreira Rodrigues,[2] S. Ferreres Sole,[29] M. Ferro-Luzzi,[44] S. Filippov,[38] R. A. Fini,[16] M. Fiorini,[18,f] M. Firlej,[32] C. Fitzpatrick,[44] T. Fiutowski,[32] F. Fleuret,[9,b] M. Fontana,[44] F. Fontanelli,[21,m] R. Forty,[44] V. Franco Lima,[56] M. Franco Sevilla,[62] M. Frank,[44] C. Frei,[44] J. Fu,[23,n] W. Funk,[44] E. Gabriel,[54] A. Gallas Torreira,[43] D. Galli,[17,c] S. Gallorini,[25] S. Gambetta,[54] Y. Gan,[3] M. Gandelman,[2] P. Gandini,[23] Y. Gao,[3] L. M. Garcia Martin,[77] J. García Pardiñas,[46] B. Garcia Plana,[43] J. Garra Tico,[51] L. Garrido,[42] D. Gascon,[42] C. Gaspar,[44] G. Gazzoni,[7] D. Gerick,[14] E. Gersabeck,[58] M. Gersabeck,[58] T. Gershon,[52] D. Gerstel,[8] Ph. Ghez,[6] V. Gibson,[51] O. G. Girard,[45] P. Gironella Gironell,[42] L. Giubega,[34] K. Gizdov,[54] V. V. Gligorov,[10] C. Göbel,[66] D. Golubkov,[36] A. Golutvin,[57,74] A. Gomes,[1,o] I. V. Gorelov,[37] C. Gotti,[22,g] E. Govorkova,[29] J. P. Grabowski,[14] R. Graciani Diaz,[42] L. A. Granado Cardoso,[44] E. Graugés,[42] E. Graverini,[45] G. Graziani,[19] A. Grecu,[34] R. Greim,[29] P. Griffith,[24] L. Grillo,[58] L. Gruber,[44] B. R. Gruberg Cazon,[59] C. Gu,[3] E. Gushchin,[38] A. Guth,[11] Yu. Guz,[41,44] T. Gys,[44] T. Hadavizadeh,[59] C. Hadjivasiliou,[7] G. Haefeli,[45] C. Haen,[44] S. C. Haines,[51] B. Hamilton,[62] Q. Han,[69] X. Han,[14] T. H. Hancock,[59] S. Hansmann-Menzemer,[14] N. Harnew,[59] T. Harrison,[56] C. Hasse,[44] M. Hatch,[44] J. He,[4] M. Hecker,[57] K. Heijhoff,[29] K. Heinicke,[12] A. Heister,[12] K. Hennessy,[56] L. Henry,[77] M. Heß,[71] J. Heuel,[11] A. Hicheur,[65] R. Hidalgo Charman,[58] D. Hill,[59] M. Hilton,[58] P. H. Hopchev,[45] J. Hu,[14] W. Hu,[69] W. Huang,[4] Z. C. Huard,[61] W. Hulsbergen,[29] T. Humair,[57] M. Hushchyn,[75] D. Hutchcroft,[56] D. Hynds,[29] P. Ibis,[12] M. Idzik,[32] P. Ilten,[49] A. Inglessi,[35] A. Inyakin,[41] K. Ivshin,[35] R. Jacobsson,[44] S. Jakobsen,[44] J. Jalocha,[59] E. Jans,[29] B. K. Jashal,[77] A. Jawahery,[62] F. Jiang,[3] M. John,[59] D. Johnson,[44] C. R. Jones,[51] C. Joram,[44] B. Jost,[44] N. Jurik,[59] S. Kandybei,[47] M. Karacson,[44] J. M. Kariuki,[50] S. Karodia,[55] N. Kazeev,[75] M. Kecke,[14] F. Keizer,[51] M. Kelsey,[64] M. Kenzie,[51] T. Ketel,[30] B. Khanji,[44] A. Kharisova,[76] C. Khurewathanakul,[45] K. E. Kim,[64]

T. Kirn,[11] V. S. Kirsebom,[45] S. Klaver,[20] K. Klimaszewski,[33] S. Koliiev,[48] M. Kolpin,[14] A. Kondybayeva,[74] A. Konoplyannikov,[36] P. Kopciewicz,[32] R. Kopecna,[14] P. Koppenburg,[29] I. Kostiuk,[29,48] O. Kot,[48] S. Kotriakhova,[35] M. Kozeiha,[7] L. Kravchuk,[38] M. Kreps,[52] F. Kress,[57] S. Kretzschmar,[11] P. Krokovny,[40,e] W. Krupa,[32] W. Krzemien,[33] W. Kucewicz,[31,p] M. Kucharczyk,[31] V. Kudryavtsev,[40,e] G. J. Kunde,[63] A. K. Kuonen,[45] T. Kvaratskheliya,[36] D. Lacarrere,[44] G. Lafferty,[58] A. Lai,[24] D. Lancierini,[46] G. Lanfranchi,[20] C. Langenbruch,[11] T. Latham,[52] C. Lazzeroni,[49] R. Le Gac,[8] R. Lefèvre,[7] A. Leflat,[37] F. Lemaitre,[44] O. Leroy,[8] T. Lesiak,[31] B. Leverington,[14] H. Li,[67] P.-R. Li,[4,q] X. Li,[63] Y. Li,[5] Z. Li,[64] X. Liang,[64] T. Likhomanenko,[73] R. Lindner,[44] F. Lionetto,[46] V. Lisovskyi,[9] G. Liu,[67] X. Liu,[3] D. Loh,[52] A. Loi,[24] J. Lomba Castro,[43] I. Longstaff,[55] J. H. Lopes,[2] G. Loustau,[46] G. H. Lovell,[51] D. Lucchesi,[25,r] M. Lucio Martinez,[43] Y. Luo,[3] A. Lupato,[25] E. Luppi,[18,f] O. Lupton,[52] A. Lusiani,[26,u] X. Lyu,[4] F. Machefert,[9] F. Maciuc,[34] V. Macko,[45] P. Mackowiak,[12] S. Maddrell-Mander,[50] O. Maev,[35,44] K. Maguire,[58] D. Maisuzenko,[35] M. W. Majewski,[32] S. Malde,[59] B. Malecki,[44] A. Malinin,[73] T. Maltsev,[40,e] H. Malygina,[14] G. Manca,[24,s] G. Mancinelli,[8] D. Marangotto,[23,n] J. Maratas,[7,t] J. F. Marchand,[6] U. Marconi,[17] C. Marin Benito,[9] M. Marinangeli,[45] P. Marino,[45] J. Marks,[14] P. J. Marshall,[56] G. Martellotti,[28] L. Martinazzoli,[44] M. Martinelli,[44,22,g] D. Martinez Santos,[43] F. Martinez Vidal,[77] A. Massafferri,[1] M. Materok,[11] R. Matev,[44] A. Mathad,[46] Z. Mathe,[44] V. Matiunin,[36] C. Matteuzzi,[22] K. R. Mattioli,[78] A. Mauri,[46] E. Maurice,[9,b] B. Maurin,[45] M. McCann,[57,44] A. McNab,[58] R. McNulty,[15] J. V. Mead,[56] B. Meadows,[61] C. Meaux,[8] N. Meinert,[71] D. Melnychuk,[33] M. Merk,[29] A. Merli,[23,n] E. Michielin,[25] D. A. Milanes,[70] E. Millard,[52] M.-N. Minard,[6] O. Mineev,[36] L. Minzoni,[18,f] D. S. Mitzel,[14] A. Mödden,[12] A. Mogini,[10] R. D. Moise,[57] T. Mombächer,[12] I. A. Monroy,[70] S. Monteil,[7] M. Morandin,[25] G. Morello,[20] M. J. Morello,[26,u] J. Moron,[32] A. B. Morris,[8] R. Mountain,[64] H. Mu,[3] F. Muheim,[54] M. Mukherjee,[69] M. Mulder,[29] D. Müller,[44] J. Müller,[12] K. Müller,[46] V. Müller,[12] C. H. Murphy,[59] D. Murray,[58] P. Naik,[50] T. Nakada,[45] R. Nandakumar,[53] A. Nandi,[59] T. Nanut,[45] I. Nasteva,[2] M. Needham,[54] N. Neri,[23,n] S. Neubert,[14] N. Neufeld,[44] R. Newcombe,[57] T. D. Nguyen,[45] C. Nguyen-Mau,[45,v] S. Nieswand,[11] R. Niet,[12] N. Nikitin,[37] N. S. Nolte,[44] A. Oblakowska-Mucha,[32] V. Obraztsov,[41] S. Ogilvy,[55] D. P. O'Hanlon,[17] R. Oldeman,[24,s] C. J. G. Onderwater,[72] J. D. Osborn,[78] A. Ossowska,[31] J. M. Otalora Goicochea,[2] T. Ovsiannikova,[36] P. Owen,[46] A. Oyanguren,[77] P. R. Pais,[45] T. Pajero,[26,u] A. Palano,[16] M. Palutan,[20] G. Panshin,[76] A. Papanestis,[53] M. Pappagallo,[54] L. L. Pappalardo,[18,f] W. Parker,[62] C. Parkes,[58,44] G. Passaleva,[19,44] A. Pastore,[16] M. Patel,[57] C. Patrignani,[17,c] A. Pearce,[44] A. Pellegrino,[29] G. Penso,[28] M. Pepe Altarelli,[44] S. Perazzini,[17] D. Pereima,[36] P. Perret,[7] L. Pescatore,[45] K. Petridis,[50] A. Petrolini,[21,m] A. Petrov,[73] S. Petrucci,[54] M. Petruzzo,[23,n] B. Pietrzyk,[6] G. Pietrzyk,[45] M. Pikies,[31] M. Pili,[59] D. Pinci,[28] J. Pinzino,[44] F. Pisani,[44] A. Piucci,[14] V. Placinta,[34] S. Playfer,[54] J. Plews,[49] M. Plo Casasus,[43] F. Polci,[10] M. Poli Lener,[20] M. Poliakova,[64] A. Poluektov,[8] N. Polukhina,[74,w] I. Polyakov,[64] E. Polycarpo,[2] G. J. Pomery,[50] S. Ponce,[44] A. Popov,[41] D. Popov,[49] S. Poslavskii,[41] E. Price,[50] C. Prouve,[43] V. Pugatch,[48] A. Puig Navarro,[46] H. Pullen,[59] G. Punzi,[26,i] W. Qian,[4] J. Qin,[4] R. Quagliani,[10] B. Quintana,[7] N. V. Raab,[15] B. Rachwal,[32] J. H. Rademacker,[50] M. Rama,[26] M. Ramos Pernas,[43] M. S. Rangel,[2] F. Ratnikov,[39,75] G. Raven,[30] M. Ravonel Salzgeber,[44] M. Reboud,[6] F. Redi,[45] S. Reichert,[12] F. Reiss,[10] C. Remon Alepuz,[77] Z. Ren,[3] V. Renaudin,[59] S. Ricciardi,[53] S. Richards,[50] K. Rinnert,[56] P. Robbe,[9] A. Robert,[10] A. B. Rodrigues,[45] E. Rodrigues,[61] J. A. Rodriguez Lopez,[70] M. Roehrken,[44] S. Roiser,[44] A. Rollings,[59] V. Romanovskiy,[41] A. Romero Vidal,[43] J. D. Roth,[78] M. Rotondo,[20] M. S. Rudolph,[64] T. Ruf,[44] J. Ruiz Vidal,[77] J. J. Saborido Silva,[43] N. Sagidova,[35] B. Saitta,[24,s] V. Salustino Guimaraes,[66] C. Sanchez Gras,[29] C. Sanchez Mayordomo,[77] B. Sanmartin Sedes,[43] R. Santacesaria,[28] C. Santamarina Rios,[43] M. Santimaria,[20,44] E. Santovetti,[27,x] G. Sarpis,[58] A. Sarti,[20,y] C. Satriano,[28,z] A. Satta,[27] M. Saur,[4] D. Savrina,[36,37] S. Schael,[11] M. Schellenberg,[12] M. Schiller,[55] H. Schindler,[44] M. Schmelling,[13] T. Schmelzer,[12] B. Schmidt,[44] O. Schneider,[45] A. Schopper,[44] H. F. Schreiner,[61] M. Schubiger,[29] S. Schulte,[45] M. H. Schune,[9] R. Schwemmer,[44] B. Sciascia,[20] A. Sciubba,[28,y] A. Semennikov,[36] E. S. Sepulveda,[10] A. Sergi,[49,44] N. Serra,[46] J. Serrano,[8] L. Sestini,[25] A. Seuthe,[12] P. Seyfert,[44] M. Shapkin,[41] T. Shears,[56] L. Shekhtman,[40,e] V. Shevchenko,[73] E. Shmanin,[74] B. G. Siddi,[18] R. Silva Coutinho,[46] L. Silva de Oliveira,[2] G. Simi,[25,r] S. Simone,[16,k] I. Skiba,[18] N. Skidmore,[14] T. Skwarnicki,[64] M. W. Slater,[49] J. G. Smeaton,[51] E. Smith,[11] I. T. Smith,[54] M. Smith,[57] M. Soares,[17] l. Soares Lavra,[1] M. D. Sokoloff,[61] F. J. P. Soler,[55] B. Souza De Paula,[2] B. Spaan,[12] E. Spadaro Norella,[23,n] P. Spradlin,[55] F. Stagni,[44] M. Stahl,[14] S. Stahl,[44] P. Stefko,[45] S. Stefkova,[57] O. Steinkamp,[46] S. Stemmle,[14] O. Stenyakin,[41] M. Stepanova,[35] H. Stevens,[12] A. Stocchi,[9] S. Stone,[64] S. Stracka,[26] M. E. Stramaglia,[45] M. Straticiuc,[34] U. Straumann,[46] S. Strokov,[76] J. Sun,[3] L. Sun,[68] Y. Sun,[62] K. Swientek,[32] A. Szabelski,[33] T. Szumlak,[32] M. Szymanski,[4] Z. Tang,[3] T. Tekampe,[12] G. Tellarini,[18] F. Teubert,[44] E. Thomas,[44] M. J. Tilley,[57] V. Tisserand,[7] S. T'Jampens,[6] M. Tobin,[5] S. Tolk,[44] L. Tomassetti,[18,f] D. Tonelli,[26] D. Y. Tou,[10] E. Tournefier,[6] M. Traill,[55] M. T. Tran,[45] A. Trisovic,[51] A. Tsaregorodtsev,[8] G. Tuci,[26,44,i]

A. Tully,[51] N. Tuning,[29] A. Ukleja,[33] A. Usachov,[9] A. Ustyuzhanin,[39,75] U. Uwer,[14] A. Vagner,[76] V. Vagnoni,[17] A. Valassi,[44] S. Valat,[44] G. Valenti,[17] M. van Beuzekom,[29] H. Van Hecke,[63] E. van Herwijnen,[44] C. B. Van Hulse,[15] J. van Tilburg,[29] M. van Veghel,[29] R. Vazquez Gomez,[44] P. Vazquez Regueiro,[43] C. Vázquez Sierra,[29] S. Vecchi,[18] J. J. Velthuis,[50] M. Veltri,[19,aa] A. Venkateswaran,[64] M. Vernet,[7] M. Veronesi,[29] M. Vesterinen,[52] J. V. Viana Barbosa,[44] D. Vieira,[4] M. Vieites Diaz,[43] H. Viemann,[71] X. Vilasis-Cardona,[42,h] A. Vitkovskiy,[29] M. Vitti,[51] V. Volkov,[37] A. Vollhardt,[46] D. Vom Bruch,[10] B. Voneki,[44] A. Vorobyev,[35] V. Vorobyev,[40,e] N. Voropaev,[35] R. Waldi,[71] J. Walsh,[26] J. Wang,[3] J. Wang,[5] M. Wang,[3] Y. Wang,[69] Z. Wang,[46] D. R. Ward,[51] H. M. Wark,[56] N. K. Watson,[49] D. Websdale,[57] A. Weiden,[46] C. Weisser,[60] M. Whitehead,[11] G. Wilkinson,[59] M. Wilkinson,[64] I. Williams,[51] M. Williams,[60] M. R. J. Williams,[58] T. Williams,[49] F. F. Wilson,[53] M. Winn,[9] W. Wislicki,[33] M. Witek,[31] G. Wormser,[9] S. A. Wotton,[51] K. Wyllie,[44] Z. Xiang,[4] D. Xiao,[69] Y. Xie,[69] H. Xing,[67] A. Xu,[3] L. Xu,[3] M. Xu,[69] Q. Xu,[4] Z. Xu,[6] Z. Xu,[3] Z. Yang,[3] Z. Yang,[62] Y. Yao,[64] L. E. Yeomans,[56] H. Yin,[69] J. Yu,[69,bb] X. Yuan,[64] O. Yushchenko,[41] K. A. Zarebski,[49] M. Zavertyaev,[13,w] M. Zeng,[3] D. Zhang,[69] L. Zhang,[3] S. Zhang,[3] W. C. Zhang,[3,cc] Y. Zhang,[44] A. Zhelezov,[14] Y. Zheng,[4] Y. Zhou,[4] X. Zhu,[3] V. Zhukov,[11,37] J. B. Zonneveld,[54] and S. Zucchelli[17,c]

(LHCb Collaboration)

[1]*Centro Brasileiro de Pesquisas Físicas (CBPF), Rio de Janeiro, Brazil*
[2]*Universidade Federal do Rio de Janeiro (UFRJ), Rio de Janeiro, Brazil*
[3]*Center for High Energy Physics, Tsinghua University, Beijing, China*
[4]*University of Chinese Academy of Sciences, Beijing, China*
[5]*Institute Of High Energy Physics (ihep), Beijing, China*
[6]*Université Grenoble Alpes, University of Savoie Mont Blanc, CNRS, IN2P3-LAPP, Annecy, France*
[7]*Université Clermont Auvergne, CNRS/IN2P3, LPC, Clermont-Ferrand, France*
[8]*Aix Marseille Université, CNRS/IN2P3, CPPM, Marseille, France*
[9]*LAL, Université Paris-Sud, CNRS/IN2P3, Université Paris-Saclay, Orsay, France*
[10]*LPNHE, Sorbonne Université, Paris Diderot Sorbonne Paris Cité, CNRS/IN2P3, Paris, France*
[11]*I. Physikalisches Institut, RWTH Aachen University, Aachen, Germany*
[12]*Fakultät Physik, Technische Universität Dortmund, Dortmund, Germany*
[13]*Max-Planck-Institut für Kernphysik (MPIK), Heidelberg, Germany*
[14]*Physikalisches Institut, Ruprecht-Karls-Universität Heidelberg, Heidelberg, Germany*
[15]*School of Physics, University College Dublin, Dublin, Ireland*
[16]*INFN Sezione di Bari, Bari, Italy*
[17]*INFN Sezione di Bologna, Bologna, Italy*
[18]*INFN Sezione di Ferrara, Ferrara, Italy*
[19]*INFN Sezione di Firenze, Firenze, Italy*
[20]*INFN Laboratori Nazionali di Frascati, Frascati, Italy*
[21]*INFN Sezione di Genova, Genova, Italy*
[22]*INFN Sezione di Milano-Bicocca, Milano, Italy*
[23]*INFN Sezione di Milano, Milano, Italy*
[24]*INFN Sezione di Cagliari, Monserrato, Italy*
[25]*INFN Sezione di Padova, Padova, Italy*
[26]*INFN Sezione di Pisa, Pisa, Italy*
[27]*INFN Sezione di Roma Tor Vergata, Roma, Italy*
[28]*INFN Sezione di Roma La Sapienza, Roma, Italy*
[29]*Nikhef National Institute for Subatomic Physics, Amsterdam, Netherlands*
[30]*Nikhef National Institute for Subatomic Physics and VU University Amsterdam, Amsterdam, Netherlands*
[31]*Henryk Niewodniczanski Institute of Nuclear Physics Polish Academy of Sciences, Kraków, Poland*
[32]*AGH—University of Science and Technology, Faculty of Physics and Applied Computer Science, Kraków, Poland*
[33]*National Center for Nuclear Research (NCBJ), Warsaw, Poland*
[34]*Horia Hulubei National Institute of Physics and Nuclear Engineering, Bucharest-Magurele, Romania*
[35]*Petersburg Nuclear Physics Institute NRC Kurchatov Institute (PNPI NRC KI), Gatchina, Russia*
[36]*Institute of Theoretical and Experimental Physics NRC Kurchatov Institute (ITEP NRC KI), Moscow, Russia, Moscow, Russia*
[37]*Institute of Nuclear Physics, Moscow State University (SINP MSU), Moscow, Russia*
[38]*Institute for Nuclear Research of the Russian Academy of Sciences (INR RAS), Moscow, Russia*
[39]*Yandex School of Data Analysis, Moscow, Russia*
[40]*Budker Institute of Nuclear Physics (SB RAS), Novosibirsk, Russia*
[41]*Institute for High Energy Physics NRC Kurchatov Institute (IHEP NRC KI), Protvino, Russia, Protvino, Russia*

[42]ICCUB, Universitat de Barcelona, Barcelona, Spain
[43]Instituto Galego de Física de Altas Enerxías (IGFAE), Universidade de Santiago de Compostela, Santiago de Compostela, Spain
[44]European Organization for Nuclear Research (CERN), Geneva, Switzerland
[45]Institute of Physics, Ecole Polytechnique Fédérale de Lausanne (EPFL), Lausanne, Switzerland
[46]Physik-Institut, Universität Zürich, Zürich, Switzerland
[47]NSC Kharkiv Institute of Physics and Technology (NSC KIPT), Kharkiv, Ukraine
[48]Institute for Nuclear Research of the National Academy of Sciences (KINR), Kyiv, Ukraine
[49]University of Birmingham, Birmingham, United Kingdom
[50]H.H. Wills Physics Laboratory, University of Bristol, Bristol, United Kingdom
[51]Cavendish Laboratory, University of Cambridge, Cambridge, United Kingdom
[52]Department of Physics, University of Warwick, Coventry, United Kingdom
[53]STFC Rutherford Appleton Laboratory, Didcot, United Kingdom
[54]School of Physics and Astronomy, University of Edinburgh, Edinburgh, United Kingdom
[55]School of Physics and Astronomy, University of Glasgow, Glasgow, United Kingdom
[56]Oliver Lodge Laboratory, University of Liverpool, Liverpool, United Kingdom
[57]Imperial College London, London, United Kingdom
[58]School of Physics and Astronomy, University of Manchester, Manchester, United Kingdom
[59]Department of Physics, University of Oxford, Oxford, United Kingdom
[60]Massachusetts Institute of Technology, Cambridge, Massachusetts, USA
[61]University of Cincinnati, Cincinnati, Ohio, USA
[62]University of Maryland, College Park, Maryland, USA
[63]Los Alamos National Laboratory (LANL), Los Alamos, New Mexico, USA
[64]Syracuse University, Syracuse, New York, USA
[65]Laboratory of Mathematical and Subatomic Physics, Constantine, Algeria
[associated with Universidade Federal do Rio de Janeiro (UFRJ), Rio de Janeiro, Brazil]
[66]Pontifícia Universidade Católica do Rio de Janeiro (PUC-Rio), Rio de Janeiro, Brazil
[associated with Universidade Federal do Rio de Janeiro (UFRJ), Rio de Janeiro, Brazil]
[67]South China Normal University, Guangzhou, China
(associated with Center for High Energy Physics, Tsinghua University, Beijing, China)
[68]School of Physics and Technology, Wuhan University, Wuhan, China
(associated with Center for High Energy Physics, Tsinghua University, Beijing, China)
[69]Institute of Particle Physics, Central China Normal University, Wuhan, Hubei, China
(associated with Center for High Energy Physics, Tsinghua University, Beijing, China)
[70]Departamento de Fisica, Universidad Nacional de Colombia, Bogota, Colombia
(associated with LPNHE, Sorbonne Université, Paris Diderot Sorbonne Paris Cité, CNRS/IN2P3, Paris, France)
[71]Institut für Physik, Universität Rostock, Rostock, Germany
(associated with Physikalisches Institut, Ruprecht-Karls-Universität Heidelberg, Heidelberg, Germany)
[72]Van Swinderen Institute, University of Groningen, Groningen, Netherlands
(associated with Nikhef National Institute for Subatomic Physics, Amsterdam, Netherlands)
[73]National Research Centre Kurchatov Institute, Moscow, Russia
[associated with Institute of Theoretical and Experimental Physics NRC Kurchatov Institute (ITEP NRC KI), Moscow, Russia, Moscow, Russia]
[74]National University of Science and Technology "MISIS", Moscow, Russia
[associated with Institute of Theoretical and Experimental Physics NRC Kurchatov Institute (ITEP NRC KI), Moscow, Russia, Moscow, Russia]
[75]National Research University Higher School of Economics, Moscow, Russia
(associated with Yandex School of Data Analysis, Moscow, Russia)
[76]National Research Tomsk Polytechnic University, Tomsk, Russia
[associated with Institute of Theoretical and Experimental Physics NRC Kurchatov Institute (ITEP NRC KI), Moscow, Russia, Moscow, Russia]
[77]Instituto de Fisica Corpuscular, Centro Mixto Universidad de Valencia—CSIC, Valencia, Spain
(associated with Institution #42)
[78]University of Michigan, Ann Arbor, USA
(associated with Syracuse University, Syracuse, New York, USA)

[a]Deceased.
[b]Also at Laboratoire Leprince-Ringuet, Palaiseau, France.
[c]Also at Università di Bologna, Bologna, Italy.
[d]Also at Università di Modena e Reggio Emilia, Modena, Italy.
[e]Also at Novosibirsk State University, Novosibirsk, Russia.

[f]Also at Università di Ferrara, Ferrara, Italy.
[g]Also at Università di Milano Bicocca, Milano, Italy.
[h]Also at LIFAELS, La Salle, Universitat Ramon Llull, Barcelona, Spain.
[i]Also at Università di Pisa, Pisa, Italy.
[j]Also at H.H. Wills Physics Laboratory, University of Bristol, Bristol, United Kingdom.
[k]Also at Università di Bari, Bari, Italy.
[l]Also at Sezione INFN di Trieste, Trieste, Italy.
[m]Also at Università di Genova, Genova, Italy.
[n]Also at Università degli Studi di Milano, Milano, Italy.
[o]Also at Universidade Federal do Triângulo Mineiro (UFTM), Uberaba-MG, Brazil.
[p]Also at AGH—University of Science and Technology, Faculty of Computer Science, Electronics and Telecommunications, Kraków, Poland.
[q]Also at Lanzhou University, Lanzhou, China.
[r]Also at Università di Padova, Padova, Italy.
[s]Also at Università di Cagliari, Cagliari, Italy.
[t]Also at MSU—Iligan Institute of Technology (MSU-IIT), Iligan, Philippines.
[u]Also at Scuola Normale Superiore, Pisa, Italy.
[v]Also at Hanoi University of Science, Hanoi, Vietnam.
[w]Also at P.N. Lebedev Physical Institute, Russian Academy of Science (LPI RAS), Moscow, Russia.
[x]Also at Università di Roma Tor Vergata, Roma, Italy.
[y]Also at Università di Roma La Sapienza, Roma, Italy.
[z]Also at Università della Basilicata, Potenza, Italy.
[aa]Also at Università di Urbino, Urbino, Italy.
[bb]Also at Physics and Micro Electronic College, Hunan University, Changsha City, China.
[cc]Also at School of Physics and Information Technology, Shaanxi Normal University (SNNU), Xi'an, China.